ACS APPLIED MATERIALS & INTERFACES

Research Article

www.acsami.org

Superior Mechanical Properties of Epoxy Composites Reinforced by 3D Interconnected Graphene Skeleton

Ya Ni, Lei Chen, Kunyue Teng, Jie Shi, Xiaoming Qian, Zhiwei Xu,* Xu Tian, Chuansheng Hu, and Meijun Ma

Key Laboratory of Advanced Braided Composites, Ministry of Education, School of Textiles, Tianjin Polytechnic University, Tianjin 300387, P. R. China

Supporting Information

ABSTRACT: Epoxy-based composites reinforced by three-dimensional graphene skeleton (3DGS) were fabricated in resin transfer molding method with respect to the difficulty in good dispersion and arrangement of graphene sheets in composites by directly mixing graphene and epoxy. 3DGS was synthesized in the process of self-assembly and reduction with poly(amidoamine) dendrimers. In the formation of 3DGS, graphene sheets were in good dispersion and ordered state, which resulted in exceptional mechanical properties and thermal stability for epoxy composites. For 3DGS/epoxy composites, the tensile and compressive strengths significantly increased by 120.9% and 148.3%, respectively, as well as the glass transition temperature, which increased by a notable 19 °C, unlike the thermal exfoliation graphene/epoxy composites via direct-mixing route, which increased by only 0.20 wt % content of fillers. Relative to the graphene/epoxy composites in direct-mixing method mentioned in literature, the increase in tensile and compressive strengths of 3DGS/epoxy composites was at least twofold and sevenfold, respectively. It can be expected that 3DGS, which comes from preforming graphene sheets orderly and dispersedly, would replace graphene nanosheets in polymer nanocomposite reinforcement and endow composites with unique structure and some unexpected performance.

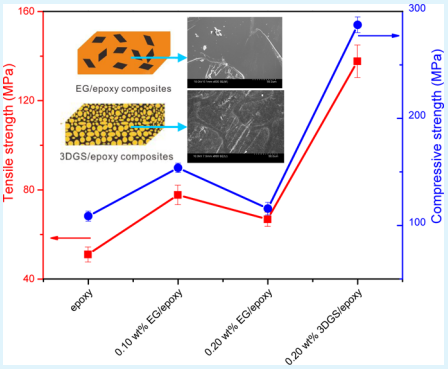

KEYWORDS: *three-dimensional graphene skeleton, epoxy-based composites, ordered arrangement, resin transfer molding, mechanical properties*

1. INTRODUCTION

Graphene, with one-atom thick and two-dimensional (2D) sheet of sp^2-bonded carbon, has a range of excellent properties.[1,2] Since Geim et al. peeled a few graphene sheets from highly crystalline graphite by a "scotch tape" method in 2004,[3] some unique properties of this conceptual matter have been found and indicate potential applications in nanocomposites with various matrixes, ultrathin membrane materials, etc.[4] Owing to its exceptional physical properties, such as high surface area, excellent thermal conductivity, extremely high mechanical flexibility, and electrical conductivity, graphene has attracted tremendous research interest in recent years.[5−8] The reliable and scaled-up production of graphene derivatives, such as graphene oxide and reduced graphene oxide, offers a wide range of possibilities to synthesize graphene-based functional materials for various applications. These excellent characteristics have brought great achievements in design of novel graphene functional materials with tailored properties.[9]

Individual graphene sheet has prominent mechanical properties, and a single-layered graphene is found to exhibit extraordinary Young's modulus of 1100 GPa and tensile strength of 130 GPa.[10,11] These characteristics make them ideal fillers for polymer nanocomposites that were used in advanced materials.[1,12] Thus, incorporating graphene sheets into composite materials is one feasible route to harness these properties for applications.[8,11] In the past few years, graphene sheets have been introduced into a wide range of polymer matrix, including epoxy, polystyrene, polypropylene, and so on, for various functional materials.[13] Epoxy, one of the most important thermosetting polymers, is used in widespread fields. Numerous attempts such as mixing epoxy polymers with a second phase of superior nanofillers (nanospheres, nanotubes, nanoplatelets, etc.) and their combination have been made to improve the toughness, stiffness, and strength and to endow the multifunctional properties.[14] Graphene/polymer composites are mostly prepared with the methods of solvent mixing and in situ polymerization, which often consume large amounts of organic solvents. However, the bottleneck is that graphene or graphene oxide sheets tend to form severe aggregations in composites due to the strong van der Waals forces among them, which limits load transfer from the matrix to the sheets.[15] The strong van der Waals force between the fillers results in uneven dispersion, and consequently, the properties of composites fall short of the expectations. Thus, to achieve

Received: March 23, 2015
Accepted: May 7, 2015
Published: May 7, 2015

DOI: 10.1021/acsami.5b02552
ACS Appl. Mater. Interfaces 2015, 7, 11583−11591

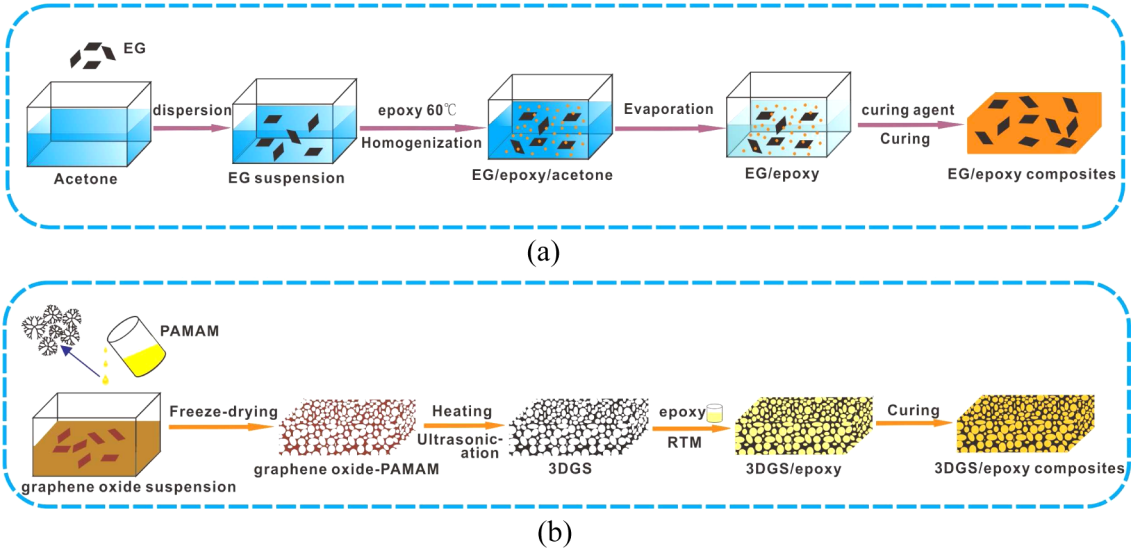

Figure 1. Flowchart for the fabrication process of EG/epoxy composites (a) and 3DGS/epoxy composites (b).

optimal enhancement in the properties of graphene/polymer composites, several key issues should be resolved, namely, improved dispersion and exfoliation of graphene,[16] alignment of graphene in polymer,[17,18] surface modification of graphene, and interfacial adhesion with the matrix.[19,20] On one hand, different dispersion methods as well as filler surface functionalization and the use of a variety of dispersing agents were developed to overcome these challenges.[21] Tremendous approaches have also been exploited to functionalize graphene or graphene oxide sheets to fabricate derivatives, which may improve their compatibility in a polymeric matrix. Unfortunately, these methods are still unable to significantly improve the performance of polymer composites. Homogeneous and stable dispersion of the nanofillers in the polymer matrix to enhance the comprehensive performance of composites remain critical challenges in this field.[22] On the other hand, alignment and rational assembly of graphene sheets have attracted a great deal of attention for the preparation of composite materials.[23] In this regard, some methods have been studied, such as electrical/magnetic fields or mechanical shear.[24] However, the process can be difficult to achieve, and graphene sheets are in the in-plane direction, which retains aligned morphology as well as limits final applications.[22,23] Moreover, the improvement of the overall performance of composite materials is considerably restricted. Hence, to realize reasonable and orderly arrangement of graphene in polymer composites is still a huge challenge for the fabrication of high-performance and multifunctional composites.

To improve the dispersion and orientation of graphene sheets, efforts have been made to assemble individual graphene sheets into three-dimensional (3D) graphene network materials such as hydrogels,[25] aerogels,[5,26] and macroporous films.[27] Current methods to prepare 3D graphene macrostructures involve template-directing method,[28,29] cross-linking method,[30] directed chemical vapor deposition,[31] and in situ reduction assembly method.[32] These 3D graphene network materials have shown a thriving development due to their excellent performance, such as open porosity, high pore connectivity, large surface areas, certain strength, etc.[33] Therefore, the 3D graphene network with unique structure provides a new platform for many applications such as energy storage, supercapacitors,[34] adsorption,[35] catalysis supports,[36] and sensors.[37] Similarly, new ideas have been brought to the preparation of polymer composites. Several researchers, Jang-Kyo Kim et al.[38,39] and Kin Liao et al.,[40] have mixed 3D graphene network with polymer using a vacuum-infiltration method. Nevertheless, the performance of its composites was much less than expected on account of the insufficient in formation methods of polymer composites and the damage of cured composites in the process of etching template.

Herein, taking into account its special structure and exceptional properties, we incorporated 3D graphene network into the fabrication of epoxy-based composites as preforming reinforcement. First, 3D graphene skeleton (3DGS) was prepared by self-assembly and in situ reduction method, in which poly(amidoamine) (PAMAM) dendrimer acted as reductant and cross-linking agent. Then resin transfer molding (RTM) method was applied to fill the porous structure of 3DGS with epoxy, in which epoxy had better effect on flow patterns and infiltration under the action of external pressure compared with vacuum-infiltration method, which depended on the mobility of epoxy itself. In this way, we developed a novel method of fabricating graphene/epoxy composites, which was significantly different from traditional approach based on directly mixing graphene sheets and epoxy. It is expected that the aggregation of graphene sheets can be effectively restrained and that graphene sheets even act as ordered support structure in 3DGS/epoxy composites, which is completely different from the messy arrangement for graphene sheets in graphene/epoxy composites with direct-mixing method.

2. EXPERIMENTAL SECTION

2.1. Materials. Natural graphite flakes were supplied by Qingdao AoKe ShiMo Co. Ltd., with an average diameter of 10 μm. PAMAM was supplied by Weihai Chenyuan Co.Ltd.. Epoxy (JC-02A) with an epoxy value of 0.51−0.53 was obtained from ChangShu Jiafa Chemical Co.Ltd. Tetrahydrophthalic anhydride, which was purchased from Wenzhou Qingming Chemical, was used as the curing agent. Acetone, hydrochloric acid (HCl, 30%), potassium permanganate, concentrated sulfuric acid (H_2SO_4, 98%), and phosphoric acid (H_3PO_4, 85%) were purchased from Tianjin chemical factory and used as received.

2.2. Preparation of Three-Dimensional Graphene Skeleton. Graphite oxide was synthesized from natural graphite flakes using a

DOI: 10.1021/acsami.5b02552
ACS Appl. Mater. Interfaces 2015, 7, 11583−11591

modified Hummers method,[41,42] giving graphite oxide in a state of the pale yellow colloid. Graphene oxide was prepared from graphite oxide with ultrasonication. The concentration of graphene oxide in the suspension was determined by freeze-drying a small amount of suspension and then weighing the dried graphene oxide. PAMAM was dissolved in water and added into the graphene oxide suspension, in which graphene oxide (3 mg/mL) and PAMAM were in mass ratio of 1:1. Subsequently, the mixture was stirred for 5 min and then placed for 2 h without stirring to get homogeneous mixture. With the high-speed centrifugal process, a sticky mixture was obtained. With rapid freezing in liquid nitrogen and freeze-drying for 24 h, the porous brown solid was prepared. After heating for 12 h at 150 °C, the resulting 3DGS was fabricated in the amidation and reduction process. And intact structure of 3DGS was still maintained in the ultrasonic process for 3 h.

2.3. Fabrication of Epoxy Composites Reinforced by Three-Dimensional Graphene Skeleton and Thermal Exfoliation Graphene. Preparation of 3DGS/epoxy composites was done following the protocol as shown in Figure 1b: (1) The prepared porous 3DGS was put into the mold, which was sealed securely. (2) Epoxy with 70 wt % curing agent and 1 wt % 2-ethyl-4-methylimidazole was mixed and degassed under vacuum at 60 °C for 30 min. (3) The prepared epoxy was injected into the mold by RTM method, and epoxy was in almost constant temperature during the RTM process. (4) The mold was put into oven to cure the composites, followed by a postcuring step at 90 °C for 3 h, 120 °C for 3 h, and 150 °C for 5 h.[43] The final 3DGS/epoxy composites were prepared for the following tests.

As shown in Figure 1a, thermal exfoliation graphene (EG)/epoxy nanocomposites were prepared by dispersing EG in acetone with ultrasonication for 1 h and adding preheated epoxy. The mixture was homogenized by continued ultrasound for 3 h with the temperature of 60 °C. After acetone removal, the mixture was added with 70 wt % curing agent and 1 wt % 2-ethyl-4-methylimidazole. Then the completed curing process was performed as above.

2.4. Characterizations. Morphology and microstructure of the prepared 3DGS and fracture surface of the composites was observed with a Hitachi S-4800 field-emission scanning electron microscope (FE-SEM) at an accelerating voltage of 10 kV. The reduction process of 3DGS was determined by X-ray Diffraction (XRD, Bruker D8 Discover) with Cu Kα radiation (λ = 1.540 59 Å) with a scanning speed of 5°/min from 3 to 40° and by Fourier transform infrared spectroscopy (FTIR, Bruker Tensor 37) in the 4000−800 cm^{-1} wavenumber range. The chemical composition was analyzed by X-ray photoelectron spectroscopy (XPS, PHI 5700) with Al Kα excitation radiation. Dynamic mechanical thermal analysis (DMA) was performed on a dynamic mechanical thermal analyzer (MettlerToledo 861e instrument) in three-point bending mode at a frequency of 1 Hz with a constant heating rate of 5 °C/min ranging from 50 to 200 °C. Specimen dimensions were 60 mm × 10 mm × 4 mm. Thermal characterization of epoxy and its composite was also performed by a DSC 7 PerkinElmer instrument calibrated with indium under nitrogen atmosphere at the rate of 5 °C/min. Tensile, compressive, and flexural tests were performed to determine the effect of EG and 3DGS reinforced epoxy on the Instron mechanical testing machine, according to the ASTM D638, ASTM C365, and ASTM D790-03, respectively.

3. RESULTS AND DISCUSSION

3.1. Morphology and Structure of Three-Dimensional Graphene Skeleton. In a typical synthesis procedure of 3DGS, brown mixture of graphene oxide and PAMAM was transformed to self-assembly porous graphene oxide−PAMAM after freeze-drying. With the reduction process, a black free-standing 3D graphene skeleton was formed, which displayed a macroporous structure less than 100 μm as shown in Figure 2. The distorted graphene sheets were randomly cross-linked with rich micropores interpenetrating inside, and the surface area of 3DGS was up to 202 m^2/g.[35,37] Under the mixing and

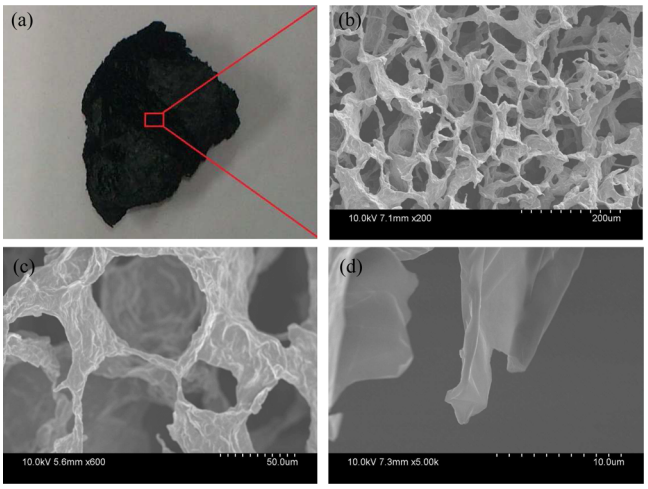

Figure 2. (a) Digital image of 3DGS. (b, c) FE-SEM images at different magnifications and (d) broken end of 3DGS.

dehydration process of graphene oxide and PAMAM, the mixture was formed into a microporous monolithic graphene oxide−PAMAM, in which PAMAM played a supporting role. Graphene sheets were to be cross-linked with dendrimer structure caused by thermal reduction in vacuum, in which PAMAM had good reactivity and compatibilization effect due to the multiple end-reactive groups. Under the action of chemical bonds between the graphene sheets and PAMAM, the graphene sheets were inhibited to be restacked and formed a 3D graphene skeleton with open micropores.[44] To bear out the stability of this porous structure, 3D graphene skeleton was in ultrasonic processing for 3 h with the solvent of *N*,*N*-dimethylformamide, which could disperse graphene sheets and thermally treated PAMAM. The 3DGS was free of damage after ultrasonic treatment (Supporting Information, Figure S2), which indicated that chemical bonds were in existence between graphene sheets and PAMAM. As the structure was supported by assembled graphene sheets, there was noticeable fold on graphene sheets.

XRD is a powerful tool to characterize the structural quality of graphite oxide, graphene oxide−PAMAM, and 3DGS materials, as shown in Figure 3, which reveals the information

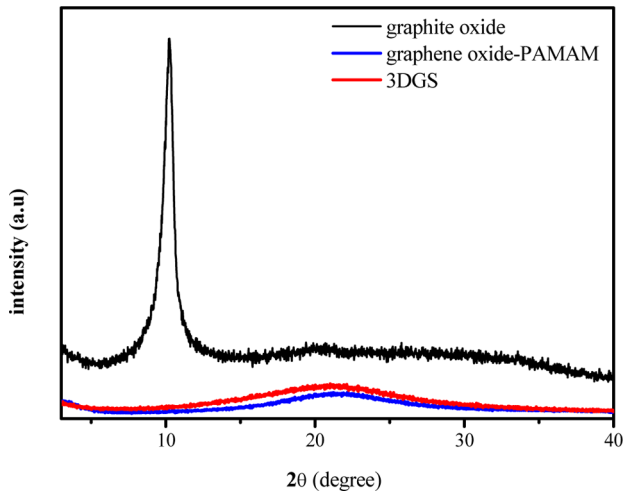

Figure 3. XRD patterns of graphite oxide, graphene oxide−PAMAM, and 3DGS.

DOI: 10.1021/acsami.5b02552
ACS Appl. Mater. Interfaces 2015, 7, 11583−11591

on the structural evolutions. The XRD pattern of graphite oxide exhibited a layer-to-layer stacking distance of 0.81 nm, corresponding to a typical diffraction peak at 2θ of 10.8°, pointing to an ordered structure.[42] However, with the process of sonication for graphite oxide and mixing with PAMAM, the characteristic peak of graphite oxide did not appear in the pattern of the graphene oxide−PAMAM sample, clearly indicating that the graphite oxide was fully exfoliated into graphene oxide sheets and that dendrimer PAMAM molecules were well-dispersed in graphene oxide solution and mixed evenly with graphene oxide sheets.[45,46] Nevertheless, the disappearance of the peak at 10.8° was also a mark for the reduction of graphene oxide in the graphene oxide−PAMAM sample.[47−49] As shown in Supporting Information, graphene oxide separated from graphene oxide−PAMAM sample was partially reduced due to the amine groups in PAMAM, which was confirmed by XPS and XRD (Supporting Information, Figure S1). For the macroscopic condition of graphene oxide−PAMAM, it gave a porous structure after the process of freeze-drying. Probably, graphene oxide sheets contacted one another due to $\pi-\pi$ stacking and hydrogen bonding on one hand; on the other hand PAMAM monomers adsorbed on the surface of graphene oxide sheets via favorable interactions (e.g., hydrogen bonding) between the amines of PAMAM and oxygen-containing groups of graphene oxide in homogeneous solution of graphene oxide and PAMAM.[50] With the heating reaction in vacuum, XRD patterns of 3DGS were similar to the graphene oxide−PAMAM; this result showed a structural stability, where PAMAM played a role to support. The appearance of a broad peak from 15 to 25° may be an indication of the restacking of graphene sheets and PAMAM.

The FTIR analysis of graphite oxide and graphene oxide−PAMAM, demonstrated in Figure 4, exhibited the presence of

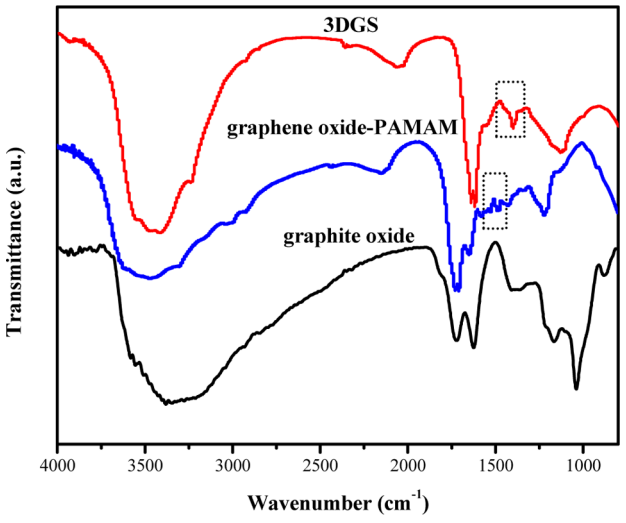

Figure 4. FTIR spectra of graphite oxide, graphene oxide−PAMAM, and 3DGS.

strong peaks corresponding to oxygen-containing groups, such as 1704 cm^{-1} (C═O stretching vibration for carbonyl and carboxylic groups) and 1620 cm^{-1}(C═C in aromatic ring). The broader peak around 3405 cm^{-1} was assigned to hydroxyl groups.[36] When water was removed by freeze-drying from the mixture of graphene oxide and PAMAM, graphene oxide−PAMAM with porous structure was obtained, and a new and tiny peak around 1570 cm^{-1} corresponding to the N−H bending vibration appeared in graphene oxide−PAMAM sample. For comparison, in the control experiment, 3DGS showed the appearance of new peak in the spectrum around 1400 cm^{-1} with heat treatment for 12 h, implying the formation of chemical bonds resulting from the reaction between the carboxylic groups and the amine groups,[51] while the peaks of oxygen-containing groups reduced significantly associated with the reduction of graphene oxide.

3.2. Structure of Three Dimensional Graphene Skeleton/Epoxy and Thermal Exfoliation Graphene/Epoxy Composites. The fabrication process for 3DGS/epoxy composites and thermal EG/epoxy composites are illustrated in Figure 1. FE-SEM images of fracture surface for 3DGS/epoxy composites and EG/epoxy composites are shown in Figure 5. Compared to EG/epoxy composites prepared via

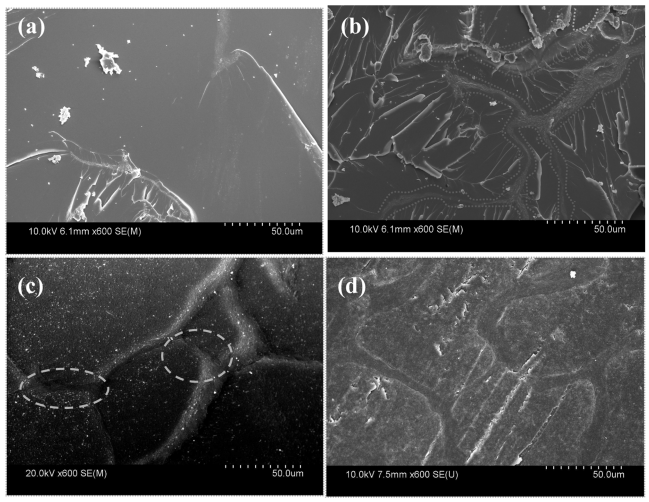

Figure 5. Fracture surface of 3DGS/epoxy composites by RTM method and EG/epoxy composites via direct-mixing route: (a) EG/epoxy composites, (b) 3DGS/epoxy composites, (c) polished fracture surface of 3DGS/epoxy composites, (d) polished fracture surface of 3DGS/epoxy composites (after etching process).

direct-mixing route (Figure 5a), the section of 3DGS/epoxy composites by RTM method (Figure 5b) was obviously rough and showed clearly successive profile. Because of the difference in hardness between graphene and epoxy, a certain height gradient appeared between the outline of 3DGS and epoxy under the process of polishing. As shown in Figure 5c, the outline structure of 3DGS in composites where there was in a bright color unfolded evidently after the polishing process. Because of the multilevel arrangement of pore structure in 3DGS, the definition of outline structure under FE-SEM varied (Figure 5c). To reveal the existing state of graphene sheets in 3DGS/epoxy composites clearly, the 3DGS was subjected to a slight etching damage with acid, and the polished surface is shown in Figure 5d. The outline structure in a dark color obviously presented between the blocks of epoxy. The outline structure was interconnected with average sizes in the range of several to dozens of micrometers, resembling the profile of the porous 3DGS.[52] As seen in Figure 5, no pores were shown between 3DGS and epoxy or even epoxy resin itself, indicating that 3DGS adhered well to epoxy matrix and that epoxy showed excellent permeability into 3DGS.[53] During the preparation of 3DGS/epoxy composites by RTM method, the interconnected 3D graphene skeleton remained intact in epoxy matrix from Figure 5, and damaged phenomenon in

DOI: 10.1021/acsami.5b02552
ACS Appl. Mater. Interfaces 2015, 7, 11583−11591

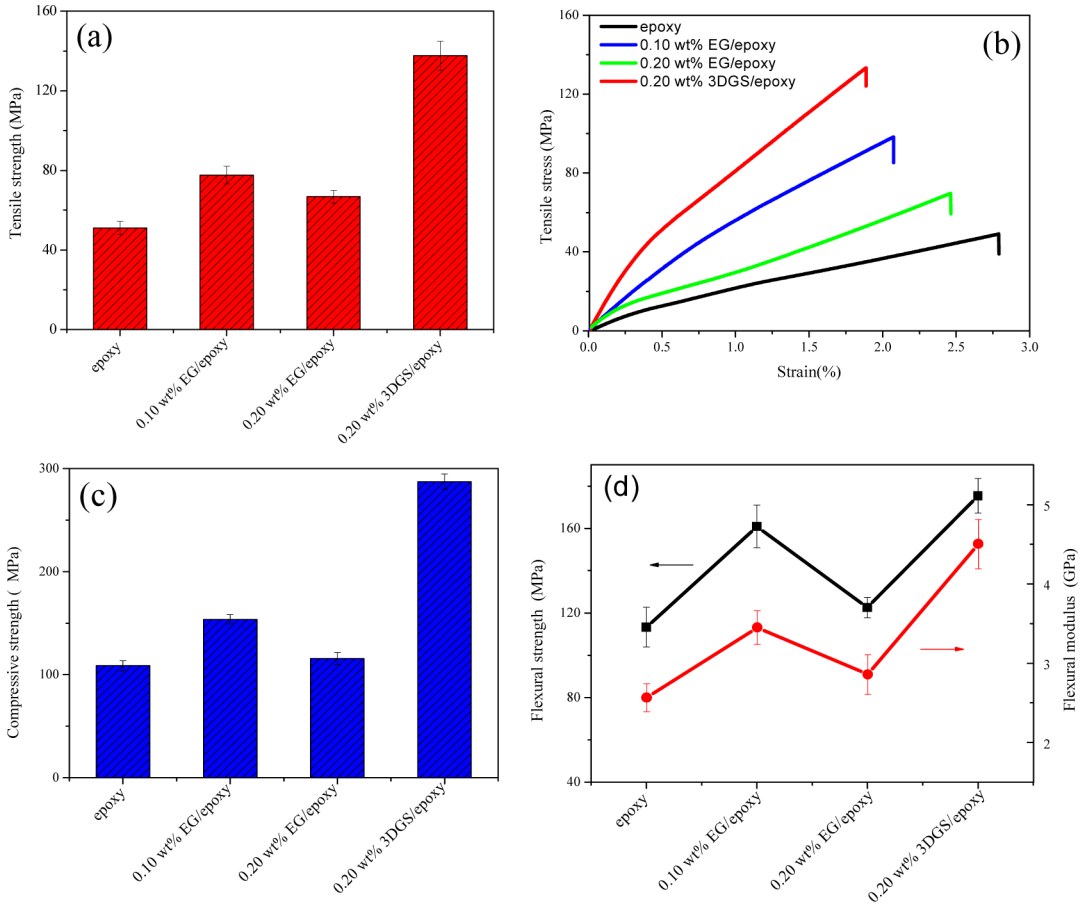

Figure 6. Mechanical properties of composites with different filler loadings: (a) tensile strength, (b) tensile stress−strain curves, (c) compressive strength, (d) flexural strength and modulus.

Table 1. Mechanical Properties of Epoxy Composites Reinforced by Graphene, Graphene Derivatives, and 3DGS

filler type	process	increase in tensile strength[a] (%)	increase in flexural modulus[a] (%)	increase in compressive strength[a] (%)	ref.
TEG	sonication	30			57
graphene	sonication	8	20		59
GNPs	stir and shear		~10	~26	60
EGNPs	sonication and shear		~7		61
graphene	sonication		~13		62
RGO	sonication and shear	~0	~12.5		63
GO	sonication and shear	~14			64
GO	shear and shear	~10			65
GO	sonication and shear	~28			15 and 55
DGEBA-f-GO	sonication and shear	~75			15
silane-f-GO	sonication and shear	~48			66
FGNs	sonication	21		14.8	67
a-TEG	sonication	43			57
FGS	sonication	0			56
G-Si	shear and shear	~24			65
GO-D230	homogenization	~25	~50		68
GAs	infiltration		<6		38
GF	infiltration		53		52
EG	sonication	39	15	16	this work
3DGS	RTM	141	75	164	this work

[a]Note: Increase (%) of mechanical properties calculated between epoxy-based composites at filler loading of 0.20 wt % and pure epoxy.

3DGS happened little, confirming the truth of 3DGS with structural integrity in a certain strength.

3.3. Mechanical Properties of Composites. On the basis of previous experiments and literature, at low EG content (<0.10 wt %), EG/epoxy composites in direct-mixing method

DOI: 10.1021/acsami.5b02552
ACS Appl. Mater. Interfaces 2015, 7, 11583−11591

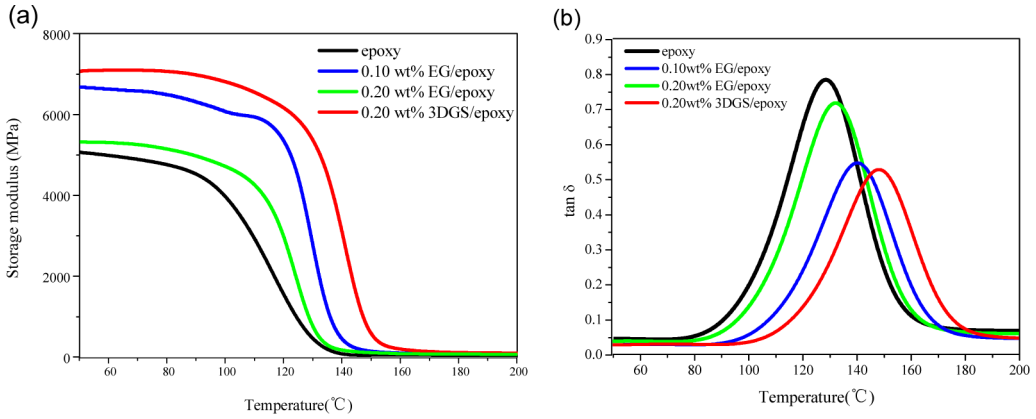

Figure 7. DMA of epoxy and its composites: (a) storage modulus (E') and (b) loss factor (tan δ).

offered significant improvement in mechanical properties.[54] For the problem of well-dispersing graphene sheets into epoxy matrix, a lot of research, including our own, has been done, which indicated optimum graphene content of ∼0.10 wt % in epoxy composites.[55−57] To ensure the superiority of 3DGS/epoxy composites and feasibility of our work, we did a comparison for the performance of composites at the same content (0.20 wt %) of EG and 3DGS. In addition, relevant research about the properties of 3DGS/epoxy composites at different content of 3DGS will be presented later in the paper.

Tensile strength and representative stress versus strain curves for neat epoxy and its composites are shown in Figure 6a,b. For EG/epoxy composites with direct-mixing method, they showed limited increase in tensile properties. The higher increase was 52.6% at EG loading of 0.10 wt %. The wrinkled surface of EG, which was at the nanoscale, may result in a strong mechanical interaction with the epoxy chains, and it may be the main reason for the enhancement of tensile properties at low EG content. And further increase in EG content reduced the tensile strength of its composites, which possibly impacted the dispersion of EG in epoxy matrix. At higher content of EG in EG/epoxy composites with direct-mixing method, the excess EG may be agglomerated, which resulted in the formation of stress concentration sites in nanocomposites.[57] When 3DGS was set as reinforcement, the resulting composites exhibited significant improvement in tensile properties. At the 3DGS loading of 0.20 wt %, tensile strength increased by 120.9% and 76.2% compared with the EG/epoxy composites in direct-mixing method at filler loading of 0.20 and 0.10 wt %, respectively. To further demonstrate their mechanical performance, the high performance of 3DGS/epoxy composites was compared with that found in other relevant literature, as shown in Table 1. Clearly, the increase of tensile strength for 3DGS/epoxy composites was at least twofold compared with epoxy-based composites reinforced by graphene and graphene derivatives via direct-mixing route mentioned in literature. The interconnected 3D graphene skeleton was a cross-linked integral by chemical bonds. To some extent, graphene sheets might be prevented to be agglomeratedin the preparation of the composites with increasing graphene content. Moreover, graphene sheets were assembled into homogeneous 3DGS as preforming reinforcement, which sharply reduced the difference in stress sites of 3DGS/epoxy composites and highlighted mechanical properties of composites.

Furthermore, to inspect the enhancing effect of 3DGS, we investigated the compressive properties of pure epoxy and its composites as shown in Figure 6c and Supporting Information, Figure S3. As the EG content increased from 0 to 0.20 wt %, a maximum compressive strength enhancement of 41.4% was obtained with EG of 0.10 wt %. Incorporation of epoxy resin into 3DGS, an important improvement in the compressive strength, was observed. The strength was increased by 148.3% and 86.9% relative to EG/epoxy composites with direct-mixing method at EG content of 0.20 and 0.10 wt %, respectively. In addition, the compressive performance of 3DGS/epoxy composites had a great advantage, ∼6 times or more, over other composites via directly mixing epoxy and graphene as listed in Table 1.

Upon the experiment about load−deflection curves, flexural strength and modulus of pure epoxy and its composites could be extracted as shown in Figure 6d and Supporting Information, Figure S4. The flexural strength of composites reinforced by EG in direct-mixing method had a maximum magnitude at 0.10 wt % of graphene content, on account of the increasing content of EG and good dispersion of fillers in nanocomposites. After more EG (0.20 wt %) was added, the flexural strength reduced. A large content of graphene maybe caused defects in the dispersion of EG into epoxy matrix. Like flexural strength, the flexural modulus for EG/epoxy composites in direct-mixing method showed highest value at EG loading of 0.10 wt %. It is well-known that the flexural strength of neat epoxy and its composites was influenced by the interfacial adhesion between fillers and epoxy matrix, whereas the composites modulus was dependent on the volume fraction of the composite constituents and modulus.[52] As shown in Figure 6d, the growth trend of flexural modulus was consistent with the flexural strength. Flexural strength and modulus revealed 43.2% and 57.3% improvement against the EG/epoxy composites based on direct mixing approach at the EG loading of 0.20 wt %.

According to the above results, excellent mechanical properties were exhibited since the introduction of 3DGS. Moreover, superior mechanical properties for 3DGS/epoxy composites were enumerated relative to epoxy-based composites reinforced by graphene and graphene derivatives in direct-mixing method, as shown in Table 1. With the ordered state of graphene sheets in 3DGS/epoxy composites shown in Figure 5, the agglomeration problem of graphene sheets at higher content in epoxy matrix had been largely improved. Simultaneously, 3DGS was an interconnected bridged structure and completely presented in epoxy composites. Unlike EG/epoxy composites in direct-mixing method, graphene sheets

DOI: 10.1021/acsami.5b02552
ACS Appl. Mater. Interfaces 2015, 7, 11583−11591

were dispersed well and assembled orderly as performing reinforcement in 3DGS/epoxy composites in this work. On the other hand, some functional groups, such as oxygen-containing groups, still existed in the resulting 3DGS from the perspective of FTIR analysis results shown in Figure 4. The interface adhesion between 3DGS and epoxy might be enhanced in the process of curing due to these functional groups, which were also conducive to the improvement of mechanical properties for 3DGS/epoxy composites.[58] Thus, 3DGS/epoxy composites by RTM method showed exceptional mechanical properties, because of the particularity of structure.

3.4. Dynamic Mechanical Thermal Properties. Dynamic mechanical spectra in the form of plots of storage modulus (E') and loss factor (tan δ) as functions of temperature are shown in Figure 7. It was seen that the storage modulus of neat epoxy and its composites was found to decrease with temperature due to the softening of the polymer chains with temperature. Addition of the 3DGS and EG, the variation tendency of storage modulus for composites, was in accordance with the change of mechanical properties. At glassy state region, the storage modulus of 3DGS/epoxy composites significantly increased compared with EG/epoxy composites based on direct mixing approach. And the starting storage modulus indicated the degree of interaction between the epoxy matrix and fillers, which reflected well the mechanical properties of the 3DGS/epoxy composites. The increased storage modulus for 3DGS/epoxy composites was due to the reinforcement and the mobility restriction of the polymer chains since the frame structure was formed between the graphene sheets in 3DGS. The temperature at which the loss factor curve showed a maximum peak was often used and recorded as the Tg.[15] From Figure 7b, the increase of Tg for 3DGS/epoxy composites to 147.5 °C suggested that the Tg of composites depended on the balance of confinement effect and the influence on curing reaction.[69] Furthermore, the variation tendency of Tg for epoxy and its composites measured by DMA (Figure 7) was consistent with that by DSC (Supporting Information, Figure S5). Summing the above, 3DGS appeared to be commendably efficient for improving the thermal stability of epoxy.

4. CONCLUSION

Regarding the difficulty in dispersion and orientation of graphene sheets in the fabrication of composites, epoxy was incorporated into 3DGS by RTM method to prepare epoxy-based composites in our work. The 3DGS was in formation of graphene sheets with a bridging effect of PAMAM in the self-assembly and reduction process, and it maintained a stable homogeneous structure in the formation of composites. Especially, the resulting 3DGS/epoxy composites exhibited superior mechanical properties and thermal stability compared with EG/epoxy composites by direct-mixing method. At the fillers loading of 0.20 wt %, the tensile and compressive strength of 3DGS/epoxy composites by RTM method increased by 120.9% and 148.3%, respectively, compared to EG/epoxy composites via direct-mixing route. Making comparison with graphene/epoxy composites via direct-mixing route in this paper and even other reports, the increment of tensile and compressive strength for 3DGS/epoxy composites was at least once and six times higher than the data reported previously. In view of the structural features of 3DGS, it can improve the graphene content, while the opportunities of aggregation for graphene sheets are out of increasing. Because of the good dispersibility and ordered arrangement for graphene sheets in 3DGS, the epoxy-based composites reinforced by 3DGS coming from preforming grahpene sheets can greatly enhance the performance of composites relative to epoxy-based composites reinforced by graphene sheets in messy arrangement. This study presents a very promising route to the fabrication of high-performance 3D graphene skeleton reinforced epoxy composites with superior mechanical properties and thermal stability.

■ ASSOCIATED CONTENT

Supporting Information

Details for the separation of graphene oxide from graphene oxide−PAMAM, XRD and XPS results of the separated graphene oxide, stable state of 3DGS with sonication in *N*,*N*-dimethylformamide, stress versus strain curves of compressive and flexural properties for epoxy and its composites, as well as DSC curves for epoxy and its composites. The Supporting Information is available free of charge on the ACS Publications website at DOI: 10.1021/acsami.5b02552.

■ AUTHOR INFORMATION

Corresponding Author

*E-mail: xuzhiwei@tjpu.edu.cn.

Notes

The authors declare no competing financial interest.

■ ACKNOWLEDGMENTS

The work was funded by the National Natural Science Foundation of China (11175130) and the Petrochemical Joint Funds of National Natural Science Fund Committee - China National Petroleum Corporation (U1362108).

■ REFERENCES

(1) Stankovich, S.; Dikin, D. A.; Dommett, G. H. B.; Kohlhaas, K. M.; Zimney, E. J.; Stach, E. A.; Piner, R. D.; Nguyen, S. T.; Ruoff, R. S. Graphene-based Composite Materials. *Nature* **2006**, *442*, 282−286.

(2) Wu, L.; Li, W.; Li, P.; Liao, S.; Qiu, S.; Chen, M.; Guo, Y.; Li, Q.; Zhu, C.; Liu, L. Powder, Paper, and Foam of Few-layer Graphene Prepared in High Yield by Electrochemical Intercalation Exfoliation of Expanded Graphite. *Small* **2014**, *10*, 1421−1429.

(3) Novoselov, K. S.; Geim, A. K. Electric Field Effect in Atomically Thin Carbon Films. *Science* **2004**, *306*, 666−669.

(4) Chen, C.; Yang, Q.-H.; Yang, Y.; Lv, W.; Wen, Y.; Hou, P.-X.; Wang, M.; Cheng, H.-M. Self-Assembled Free-Standing Graphite Oxide Membrane. *Adv. Mater.* **2009**, *21*, 3007−3011.

(5) Jiang, L.; Fan, Z. Design of Advanced Porous Graphene Materials: from Graphene Nanomesh to 3D Architectures. *Nanoscale* **2014**, *6*, 1922−1945.

(6) Zheng, Z.; Zheng, X.; Wang, H.; Du, Q. Macroporous Graphene Oxide-Polymer Composite Prepared through Pickering High Internal Phase Emulsions. *ACS Appl. Mater. Interfaces* **2013**, *5*, 7974−7482.

(7) Wu, C.; Huang, X.; Wu, X.; Qian, R.; Jiang, P. Mechanically Flexible and Multifunctional Polymer-based Graphene Foams for Elastic Conductors and Oil-Water Separators. *Adv. Mater.* **2013**, *25*, 5658−5662.

(8) Li, D.; Mueller, M. B.; Gilje, S.; Kaner, R. B.; Wallace, G. G. Processable Aqueous Dispersions of Graphene Nanosheets. *Nat. Nanotechnol.* **2008**, *3*, 101−105.

(9) Cong, H.-P.; Chen, J.-F.; Yu, S.-H. Graphene-based Macroscopic Assemblies and Architectures: an Emerging Material System. *Chem. Soc. Rev.* **2014**, *43*, 7295−7325.

(10) Changgu, L.; Xiaoding, W.; Kysar, J. W.; Hone, J. Measurements of the Elastic Properties and Intrinsic Strength of Monolayer Graphene. *Science* **2008**, *321*, 385−388.

DOI: 10.1021/acsami.5b02552
ACS Appl. Mater. Interfaces 2015, 7, 11583−11591

(11) Sun, X.; Sun, H.; Li, H.; Peng, H. Developing Polymer Composite Materials: Carbon Nanotubes or Graphene? *Adv. Mater.* **2013**, *25*, 5153−5176.
(12) Potts, J. R.; Dreyer, D. R.; Bielawski, C. W.; Ruoff, R. S. Graphene-based Polymer Nanocomposites. *Polymer* **2011**, *52*, 5−25.
(13) Tang, L.-C.; Wan, Y.-J.; Yan, D.; Pei, Y.-B.; Zhao, L.; Li, Y.-B.; Wu, L. B.; Jiang, J.-X.; Lai, G.-Q. The Effect of Graphene Dispersion on the Mechanical Properties of Graphene/epoxy Composites. *Carbon* **2013**, *60*, 16−27.
(14) Mannov, E.; Schmutzler, H.; Chandrasekaran, S.; Viets, C.; Buschhorn, S.; Toelle, F.; Muelhaupt, R.; Schulte, K. Improvement of Compressive Strength after Impact in Fibre Reinforced Polymer Composites by Matrix Modification with Thermally Reduced Graphene Oxide. *Compos. Sci. Technol.* **2013**, *87*, 36−41.
(15) Wan, Y.-J.; Tang, L.-C.; Gong, L.-X.; Yan, D.; Li, Y.-B.; Wu, L.-B.; Jiang, J.-X.; Lai, G.-Q. Grafting of Epoxy Chains onto Graphene Oxide for Epoxy Composites with Improved Mechanical and Thermal Properties. *Carbon* **2014**, *69*, 467−480.
(16) Lee, J. H.; Park, N.; Kim, B. G.; Jung, D. S.; Im, K.; Hur, J.; Choi, J. W. Restacking-Inhibited 3D Reduced Graphene Oxide for High Performance Supercapacitor Electrodes. *ACS Nano* **2013**, *7*, 9366−9374.
(17) Ansari, S.; Kelarakis, A.; Estevez, L.; Giannelis, E. P. Oriented Arrays of Graphene in a Polymer Matrix by in situ Reduction of Graphite Oxide Nanosheets. *Small* **2010**, *6*, 205−209.
(18) Xie, X. L.; Mai, Y. W.; Zhou, X. P. Dispersion and Alignment of Carbon Nanotubes in Polymer Matrix: A review. *Mater. Sci. Eng., R* **2005**, *49*, 89−112.
(19) Singh, V.; Joung, D.; Zhai, L.; Das, S.; Khondaker, S. I.; Seal, S. Graphene based Materials: Past, Present and Future. *Prog. Mater. Sci.* **2011**, *56*, 1178−1271.
(20) Prolongo, S. G.; Moriche, R.; Sanchez, M.; Urena, A. Self-stratifying and Orientation of Exfoliated Few-layer Graphene Nanoplatelets in Epoxy Composites. *Compos. Sci. Technol.* **2013**, *85*, 136−141.
(21) Yue, L.; Pircheraghi, G.; Monemian, S. A.; Manas-Zloczower, I. Epoxy Composites with Carbon Nanotubes and Graphene Nanoplatelets - Dispersion and Synergy Effects. *Carbon* **2014**, *78*, 268−278.
(22) Yousefi, N.; Lin, X.; Zheng, Q.; Shen, X.; Pothnis, J. R.; Jia, J.; Zussman, E.; Kim, J.-K. Simultaneous in situ Reduction, Self-alignment and Covalent Bonding in Graphene Oxide/epoxy Composites. *Carbon* **2013**, *59*, 406−417.
(23) Yousefi, N.; Gudarzi, M. M.; Zheng, Q.; Aboutalebi, S. H.; Sharif, F.; Kim, J.-K. Self-alignment and High Electrical Conductivity of Ultralarge Graphene Oxide-polyurethane Nanocomposites. *J. Mater. Chem.* **2012**, *22*, 12709−12717.
(24) Choi, E. S.; Brooks, J. S.; Eaton, D. L.; Al-Haik, M. S.; Hussaini, M. Y.; Garmestani, H.; Li, D.; Dahmen, K. Enhancement of Thermal and Electrical Properties of Carbon Nanotube Polymer Composites by Magnetic Field Processing. *J. Appl. Phys.* **2003**, *94*, 6034−6039.
(25) Faghihi, S.; Gheysour, M.; Karimi, A.; Salarian, R. Fabrication and Mechanical Characterization of Graphene Oxide-reinforced Poly (acrylic acid)/gelatin Composite Hydrogels. *J. Appl. Phys.* **2014**, *115*, 083513−083513.
(26) Kabiri, S.; Tran, D. N. H.; Altalhi, T.; Losic, D. Outstanding Adsorption Performance of Graphene-Carbon Nanotube Aerogels for Continuous Oil Removal. *Carbon* **2014**, *80*, 523−533.
(27) Yin, J.; Li, X.; Zhou, J.; Guo, W. Ultralight Three-Dimensional Boron Nitride Foam with Ultralow Permittivity and Superelasticity. *Nano Lett.* **2013**, *13*, 3232−3236.
(28) Ye, S.; Feng, J.; Wu, P. Deposition of Three-dimensional Graphene Aerogel on Nickel Foam as a Binder-free Supercapacitor Electrode. *ACS Appl. Mater. Interfaces* **2013**, *5*, 7122−7129.
(29) Wang, H.; Wang, G.; Ling, Y.; Qian, F.; Song, Y.; Lu, X.; Chen, S.; Tong, Y.; Li, Y. High Power Density Microbial Fuel Vell with Flexible 3D Graphene-nickel Foam as Anode. *Nanoscale* **2013**, *5*, 10283−10290.
(30) Sudeep, P. M.; Narayanan, T. N.; Ganesan, A.; Shaijumon, M. M.; Yang, H.; Ozden, S.; Patra, P. K.; Pasquali, M.; Vajtai, R.; Ganguli, S.; Roy, A. K.; Anantharaman, M. R.; Ajayan, P. M. Covalently Interconnected Three-dimensional Graphene Oxide Solids. *ACS Nano* **2013**, *7*, 7034−7040.
(31) Tang, B.; Hu, G.; Gao, H.; Shi, Z. Three-dimensional Graphene Network Assisted High Performance Dye Sensitized Solar Cells. *J. Power Sources* **2013**, *234*, 60−68.
(32) Sun, H.; Xu, Z.; Gao, C. Multifunctional, Ultra-Flyweight, Synergistically Assembled Carbon Aerogels. *Adv. Mater.* **2013**, *25*, 2554−2560.
(33) Wang, J.; Gao, L. X.; Wang, Y.; Gao, C. Novel Graphene Oxide Sponge synthesized by Freeze-drying Process for the Removal of 2,4,6-Trichlorophenol. *RSC Adv.* **2014**, *4*, 57476−57482.
(34) Yang, X.; Zhu, J.; Qiu, L.; Li, D. Bioinspired Effective Prevention of Restacking in Multilayered Graphene Films: towards the next Generation of High-performance Supercapacitors. *Adv. Mater.* **2011**, *23*, 2833−2838.
(35) Mi, X.; Huang, G.; Xie, W.; Wang, W.; Liu, Y.; Gao, J. Preparation of Graphene Oxide Aerogel and its Adsorption for Cu^{2+} Ions. *Carbon* **2012**, *50*, 4856−4864.
(36) Hailin, W.; Kakade, B. A.; Tamaki, T.; Yamaguchi, T. Synthesis of 3D Graphite Oxide-exfoliated Carbon Nanotube Carbon Composite and its Application as Catalyst Support for Fuel Cells. *J. Power Sources* **2014**, *260*, 338−348.
(37) Song, X.; Lin, L.; Rong, M.; Wang, Y.; Xie, Z.; Chen, X. Mussel-inspired, Ultralight, Multifunctional 3D Nitrogen-doped Graphene Aerogel. *Carbon* **2014**, *80*, 174−182.
(38) Wang, Z.; Shen, X.; Akbari Garakani, M.; Lin, X.; Wu, Y.; Liu, X.; Sun, X.; Kim, J. K. Graphene Aerogel/Epoxy Composites with Exceptional Anisotropic Structure and Properties. *ACS Appl. Mater. Interfaces* **2015**, *7*, 5538−5549.
(39) Jia, J.; Sun, X.; Lin, X.; Shen, X.; Mai, Y.-W.; Kim, J.-K. Exceptional Electrical Conductivity and Fracture Resistance of 3D Interconnected Graphene Foam/Epoxy Composites. *ACS Nano* **2014**, *8*, 5774−5783.
(40) Li, Y.; Samad, Y. A.; Polychronopoulou, K.; Alhassan, S. M.; Liao, K. Highly Electrically Conductive Nanocomposites Based on Polymer-Infused Graphene Sponges. *Sci. Rep* **2014**, *4*, 1−6.
(41) Marcano, D. C.; Kosynkin, D. V.; Berlin, J. M.; Sinitskii, A.; Sun, Z.; Slesarev, A.; Alemany, L. B.; Lu, W.; Tour, J. M. Improved Synthesis of Graphene Oxide. *ACS Nano* **2010**, *4*, 4806−4814.
(42) Tang, G.; Jiang, Z.-G.; Li, X.; Zhang, H.-B.; Dasari, A.; Yu, Z.-Z. Three Dimensional Graphene Aerogels and their Electrically Conductive Composites. *Carbon* **2014**, *77*, 592−599.
(43) Lei, C.; Hao, J.; Zhiwei, X.; Mingjing, S.; Xu, T.; Caiyun, Y.; Zhen, W.; Bowen, C. A Design of Gradient Interphase Reinforced by Silanized Graphene Oxide and its Effect on Carbon Fiber/epoxy Interface. *Mater. Chem. Phys.* **2014**, *145*, 186−196.
(44) Qian, Y.; Ismail, I. M.; Stein, A. Ultralight, High-surface-area, Multifunctional Graphene-based Aerogels from Self-assembly of Graphene Oxide and Resol. *Carbon* **2014**, *68*, 221−231.
(45) Hu, J.; Kang, Z.; Li, F.; Huang, X. Graphene with Three-dimensional Architecture for High Performance Supercapacitor. *Carbon* **2014**, *67*, 221−229.
(46) Zhao, X.; Zhang, Q.; Chen, D.; Lu, P. Enhanced Mechanical Properties of Graphene-Based Poly(vinyl alcohol) Composites. *Macromolecules* **2010**, *43*, 2357−2363.
(47) Wang, D.; Li, X.; Wang, J.; Yang, J.; Geng, D.; Li, R.; Cai, M.; Sham, T.-K.; Sun, X. Defect-Rich Crystalline SnO_2 Immobilized on Graphene Nanosheets with Enhanced Cycle Performance for Li Ion Batteries. *J. Phys. Chem. C* **2012**, *116*, 22149−22156.
(48) Bao, C.; Song, L.; Xing, W.; Yuan, B.; Wilkie, C. A.; Huang, J.; Guo, Y.; Hu, Y. Preparation of Graphene by Pressurized Oxidation and Multiplex Reduction and its Polymer Nanocomposites by Master-batch-based Melt Blending. *J. Mater. Chem.* **2012**, *22*, 6088−6096.
(49) Li, Y.; Wang, J.; Li, X.; Geng, D.; Li, R.; Sun, X. Superior Energy Capacity of Graphene Nanosheets for a Nonaqueous Lithium-oxygen Battery. *Chem. Commun.* **2011**, *47*, 9438−9440.

DOI: 10.1021/acsami.5b02552
ACS Appl. Mater. Interfaces 2015, 7, 11583−11591

(50) Ye, S.; Feng, J.; Wu, P. Highly Elastic Graphene Oxide-epoxy Composite Aerogels via Simple Freeze-drying and Subsequent Routine Curing. *J. Mater. Chem. A* **2013**, *1*, 3495−3502.
(51) Wan, W.; Li, L.; Zhao, Z.; Hu, H.; Hao, X.; Winkler, D. A.; Xi, L.; Hughes, T. C.; Qiu, J. Ultrafast Fabrication of Covalently Cross-linked Multifunctional Graphene Oxide Monoliths. *Adv. Funct. Mater.* **2014**, *24*, 4915−4921.
(52) Jia, J.; Sun, X.; Lin, X.; Shen, X.; Mai, Y. W.; Kim, J. K. Exceptional Electrical Conductivity and Fracture Resistance of 3D Interconnected Graphene Foam/Epoxy Composites. *ACS Nano* **2014**, *8*, 5774−5783.
(53) Zhang, X.; Yeung, K. K.; Gao, Z.; Li, J.; Sun, H.; Xu, H.; Zhang, K.; Zhang, M.; Chen, Z.; Yuen, M. M. F.; Yang, S. Exceptional Thermal Interface Properties of a Three-dimensional Graphene Foam. *Carbon* **2014**, *6*, 201−209.
(54) Rafiee, M. A.; Rafiee, J.; Wang, Z.; Song, H.; Yu, Z.-Z.; Koratkar, N. Enhanced Mechanical Properties of Nanocomposites at Low Graphene Content. *ACS Nano* **2009**, *3*, 3884−3890.
(55) Yang, S.-Y.; Lin, W.-N.; Huang, Y.-L.; Tien, H.-W.; Wang, J.-Y.; Ma, C.-C. M.; Li, S.-M.; Wang, Y.-S. Synergetic Effects of Graphene Platelets and Carbon Nanotubes on the Mechanical and Thermal Properties of Epoxy Composites. *Carbon* **2011**, *49*, 793−803.
(56) Rafiee, M. A.; Rafiee, J.; Srivastava, I.; Wang, Z.; Song, H.; Yu, Z.-Z.; Koratkar, N. Fracture and Fatigue in Graphene Nanocomposites. *Small* **2010**, *6*, 179−183.
(57) Deng, H.; Wu, F.; Chen, L.; Xu, Z.; Liu, L.; Yang, C.; Mai, W.; Cheng, B. Enhanced Interfacial Interaction of Epoxy Nanocomposites with Activated Graphene Nanosheets. *J. Appl. Polym. Sci.* **2014**, *131*, 1−8.
(58) Liao, W. H.; Tien, H. W.; Hsiao, S. T.; Li, S. M.; Wang, Y. S.; Huang, Y. L.; Yang, S. Y.; Ma, C. C.; Wu, Y. F. Effects of Multiwalled Carbon Nanotubes Functionalization on the Morphology and Mechanical and Thermal Properties of Carbon Fiber/Vinyl Ester Composites. *ACS Appl. Mater. Interfaces* **2013**, *5*, 3975−3982.
(59) Shen, X.-J.; Liu, Y.; Xiao, H.-M.; Feng, Q.-P.; Yu, Z.-Z.; Fu, S.-Y. The Reinforcing Effect of Graphene Nanosheets on the Cryogenic Mechanical Properties of Epoxy Resins. *Compos. Sci. Technol.* **2012**, *72*, 1581−1587.
(60) Shadlou, S.; Ahmadi-Moghadam, B.; Taheri, F. The Effect of Strain-rate on the Tensile and Compressive Behavior of Graphene Reinforced Epoxy/Nanocomposites. *Mater. Des.* **2014**, *59*, 439−447.
(61) Chatterjee, S.; Wang, J. W.; Kuo, W. S.; Tai, N. H.; Salzmann, C.; Li, W. L.; Hollertz, R.; Nueesch, F. A.; Chu, B. T. T. Mechanical Reinforcement and Thermal Conductivity in Expanded Graphene Nanoplatelets Reinforced Epoxy Composites. *Chem. Phys. Lett.* **2012**, *531*, 6−10.
(62) Shokrieh, M. M.; Esmkhani, M.; Taheri-Behrooz, F.; Haghighatkhah, A. R. Displacement-controlled Flexural Bending Fatigue Behavior of Graphene/epoxy Nanocomposites. *J. Compos. Mater.* **2014**, *48*, 2935−2944.
(63) Tang, L.-C.; Wan, Y.-J.; Yan, D.; Pei, Y.-B.; Zhao, L.; Li, Y.-B.; Wu, L.-B.; Jiang, J.-X.; Lai, G.-Q. The Effect of Graphene Dispersion on the Mechanical Properties of Graphene/epoxy Composites. *Carbon* **2013**, *60*, 16−27.
(64) Ren, F.; Zhu, G.; Ren, P.; Wang, Y.; Cui, X. In situ Polymerization of Graphene Oxide and Cyanate Ester-epoxy with Enhanced Mechanical and Thermal Properties. *Appl. Surf. Sci.* **2014**, *316*, 549−557.
(65) Ahmadi-Moghadam, B.; Sharafimasooleh, M.; Shadlou, S.; Taheri, F. Effect of Functionalization of Graphene Nanoplatelets on the Mechanical Response of Graphene/epoxy Composites. *Mater. Des* **2015**, *66*, 142−149.
(66) Wan, Y.-J.; Gong, L.-X.; Tang, L.-C.; Wu, L.-B.; Jiang, J.-X. Mechanical Properties of Epoxy Composites Filled with Silane-functionalized Graphene Oxide. *Composites, Part A* **2014**, *64*, 79−89.
(67) Liu, F.; Guo, K. Reinforcing Epoxy Resin through Covalent Integration of Functionalized Graphene Nanosheets. *Polym. Adv. Technol.* **2014**, *25*, 418−423.
(68) Tang, G.; Jiang, Z.-G.; Li, X.; Zhang, H.-B.; Hong, S.; Yu, Z.-Z. Electrically Conductive Rubbery Epoxy/Diamine-functionalized Graphene Nanocomposites with Improved Mechanical Properties. *Composites, Part B* **2014**, *67*, 564−570.
(69) Wang, S.; Tambraparni, M.; Qiu, J.; Tipton, J.; Dean, D. Thermal Expansion of Graphene Composites. *Macromolecules* **2009**, *42*, 5251−5255.

DOI: 10.1021/acsami.5b02552
ACS Appl. Mater. Interfaces 2015, 7, 11583−11591